

Fig. 8. Recovered source signal $\hat{x}_2(n)$.

IV. CONCLUSION

In this correspondence, a theorem that states the condition for the existence of MIMO FIR inverses, which are also FIR inverses, is proposed and proved. The use of the theorem for equalization of a MIMO FIR channel is illustrated through a numerical example.

REFERENCES

- [1] G. Giannakis *et al.*, *Signal Processing Advances in Wireless Communications: vol I Trends in Channel Estimation and Equalization, vol II Trends in Single and Multi-User Systems*. Englewood Cliffs, NJ: PTR Prentice-Hall, 2001.
- [2] L. Tong, G. Xu, and T. Kailath, "Blind identification and equalization based on second-order statistics: A time domain approach," *IEEE Trans. Inf. Theory*, vol. 40, no. 2, pp. 340–349, Mar. 1994.
- [3] J. K. Tugnait, "Blind estimation of digital communication channel impulse response," *IEEE Trans. Commun.*, vol. 42, no. 2/3/4, pp. 1606–1616, Feb./Mar./Apr. 1994.
- [4] E. Moulines, P. Duhamel, J. Cardoso, and S. Mayrargue, "Subspace methods for the blind identification of multichannel FIR filters," *IEEE Trans. Signal Process.*, vol. 43, no. 2, pp. 516–525, Feb. 1995.
- [5] T. Kailath, *Linear Systems*. Englewood Cliffs, NJ: Prentice-Hall, 1980.
- [6] D. A. Cox, J. Little, and D. O'Shea, *Ideals, Varieties, and Algorithms*. Berlin, Germany: Springer-Verlag, 1992.

Maximum-Likelihood Estimation of Frequency and Time Offsets in OFDM Systems With Multiple Sets of Identical Data

Mu-Huo Cheng, *Member, IEEE*, and Chi-Chan Chou

Abstract—This paper generalizes the existing algorithm for the maximum-likelihood (ML) estimation of frequency and time offsets in orthogonal frequency-division multiplexing (OFDM) systems using from two sets to multiple sets of identical data. The algorithm is derived by the application of the matrix inversion lemma; the Cramér–Rao bound for estimation of the frequency offset is also obtained. For reducing realization complexity, a simplified algorithm is developed. Simulations using the ten sets of identical data in the preamble of IEEE 802.11a for estimation of frequency and time offsets have been performed to verify the effectiveness of the proposed algorithms.

Index Terms—IEEE 802.11a, maximum-likelihood (ML) estimation, orthogonal frequency-division multiplexing (OFDM).

I. INTRODUCTION

The orthogonal frequency-division-multiplexing (OFDM) scheme has been adopted in many applications such as the digital broadcast television, the wireless communications, and the high-bit-rate communications over the existing copper networks [1]–[3]. The OFDM systems, however, are highly sensitive to the frequency offset [4], [5]. Therefore, an accurate estimation of the frequency offset is critical. Existing approaches for the frequency-offset estimation using the preamble data [6], [7], the cyclic prefix data [8], [9], or the cyclostationary property [10] of the received signals have been proposed. Extensive coverage of techniques for digital synchronization is also provided in textbooks [11]–[13]. Here, we focus on the data-aided maximum-likelihood (ML) estimation in OFDM systems. The ML estimation of frequency and time offsets in OFDM systems using the two sets of identical cyclic prefix data has been derived in [8]. In the IEEE 802.11a [14] standard for wireless LAN communications, the preamble contains multiple sets of identical data for channel estimation and synchronization. Hence, an extension for the ML estimation algorithm to include for multiple sets of identical data is practically useful and worth studying. Therefore, in this paper, by using the matrix inversion lemma [15], we generalize the ML algorithm for the estimation of frequency and time offsets to include for the number of the identical data set more than two. Moreover, we also derive the Cramér–Rao bound for the frequency-offset estimate. Since the resulting ML algorithm requires high realization complexity, we further develop a simplified algorithm that can reduce significantly the realization complexity but at the cost of modest performance degradation. Simulations are then carried out to evaluate the performance of all proposed algorithms using the ten short identical symbols in the preamble of IEEE 802.11a standard.

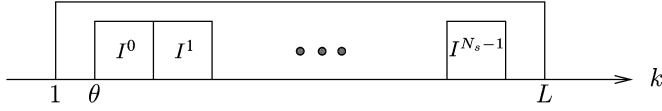
II. ALGORITHM DERIVATION

The algorithm is derived under the assumption of the nondispersive channel and the additive white Gaussian noise (AWGN) $n(k)$ with the

Manuscript received January 17, 2005; revised September 2, 2005. This work was supported by National Science Council, Taiwan, under NSC93-2213-E-009-040. The associate editor coordinating the review of this manuscript and approving it for publication was Prof. Mats Viberg.

The authors are with the Department of Electrical and Control Engineering, National Chiao Tung University, Hsinchu 30010, Taiwan (e-mail: mhcheng@cc.nctu.edu.tw; chichanchou@yahoo.com.tw).

Digital Object Identifier 10.1109/TSP.2006.874837


 Fig. 1. Observed data-encompassing contiguous N_s sets of identical data.

transmitted complex signal $s(k)$, which is also assumed to be a white Gaussian random process. The received complex sample data for a frequency offset ϵ and an integer time offset θ are given by

$$r(k) = s(k - \theta) \exp(j2\pi k\epsilon/N) + n(k) \quad (1)$$

where N represents the number of subcarriers of a complex transmitted OFDM symbol. Notice that here the effect of the offset in sampling frequency is assumed negligible such that the time offset is an integer. The effect of nonsynchronized sampling has been discussed in [16]. Suppose that we have observed L consecutive samples of $r(k)$, $k = 1, 2, \dots, L$, shown in Fig. 1, encompassing contiguous N_s sets of identical data, indexed by I^i , $i = 0, 1, \dots, N_s - 1$, where each set contains L_s data samples. Note that in theory, it is not necessary to assume that the N_s sets of identical data are contiguous. The assumption is made here for the simplicity in derivation and for the use of the preamble data in IEEE 802.11a standard. Then, the index sets are $I^i = \{\theta + iL_s, \dots, \theta + (i+1)L_s - 1\}$ for $i = 0, 1, \dots, N_s - 1$.

Collect the observed samples in the $L \times 1$ vector $\mathbf{r} = [r(1), \dots, r(L)]^T$, where the superscript T denotes the transpose operation. Notice that the samples in the N_s sets, i.e., $r(k)$, $k \in \bigcup_{i=0}^{N_s-1} I^i$, are pairwise correlated. Hence, for $m, n \in [0, N_s - 1]$, and $m \geq n$

$$\forall k \in I^0 : E[r(k + nL_s)r^*(k + mL_s)] = \begin{cases} \sigma_s^2 + \sigma_n^2, & m = n \\ \sigma_s^2 e^{-j(m-n)\epsilon'}, & (m-n) = 1, \dots, N_s - 1 \\ 0, & \text{otherwise} \end{cases} \quad (2)$$

where $E[\cdot]$ denotes the expectation, $\sigma_s^2 = E[s^2(k)]$ the signal power, $\sigma_n^2 = E[n^2(k)]$ the noise power, and $\epsilon' = 2\pi L_s \epsilon / N$.

The log-likelihood function $\Lambda(\theta, \epsilon)$ is the logarithm of $f(\mathbf{r}|\theta, \epsilon)$, the probability density function (pdf) of the L observed samples \mathbf{r} conditioned by the given time offset θ and the frequency offset ϵ . This function, by (2), can be written as

$$\begin{aligned} \Lambda(\theta, \epsilon) &= \ln f(\mathbf{r}|\theta, \epsilon) \\ &= \ln \left\{ \prod_{k \in I^0} f(r(k), r(k+L_s), \dots, r(k+(N_s-1)L_s)) \right. \\ &\quad \left. \times \prod_{k \notin \bigcup_{p=0}^{N_s-1} I^p} f(r(k)) \right\} \\ &= \ln \left\{ \prod_{k \in I^0} \frac{f(r(k), r(k+L_s), \dots, r(k+(N_s-1)L_s))}{f(r(k)) f(r(k+L_s)) \cdots f(r(k+(N_s-1)L_s))} \right. \\ &\quad \left. \times \prod_{k=1}^L f(r(k)) \right\} \quad (3) \end{aligned}$$

where the conditioned variables θ and ϵ are omitted for simplicity. Since $f(r(k))$ for each k is a one-dimensional (1-D)

zero-mean complex Gaussian distribution function, it equals $\exp[-|r(k)|^2/(\sigma_s^2 + \sigma_n^2)]/[\pi(\sigma_s^2 + \sigma_n^2)]$; the product $\prod_{k=1}^L f(r(k))$ in (3), therefore, is independent of θ and ϵ . Also the denominator in (3) equals the multiplication of N_s 1-D complex Gaussian pdf's, yielding

$$\begin{aligned} \prod_{m=0}^{N_s-1} f(r(k+mL_s)) &= \left(\frac{1}{\pi(\sigma_s^2 + \sigma_n^2)} \right)^{N_s} \\ &\quad \times \exp \left(-\frac{\sum_{m=0}^{N_s-1} |r(k+mL_s)|^2}{\sigma_s^2 + \sigma_n^2} \right) \\ &= \left(\frac{1}{\pi(\sigma_s^2 + \sigma_n^2)} \right)^{N_s} \\ &\quad \times \exp \left(-\frac{\mathbf{z}^H(k) \mathbf{z}(k)}{\sigma_s^2 + \sigma_n^2} \right) \quad (4) \end{aligned}$$

where $\mathbf{z}(k) = [r(k), r(k+L_s), \dots, r(k+(N_s-1)L_s)]^T$ and the superscript H represents the transpose conjugate (hermitian) operation. Then $f(r(k), r(k+L_s), \dots, r(k+(N_s-1)L_s)) = f(\mathbf{z}(k))$ and its pdf is an $N_s - D$ joint complex Gaussian function [17], given by

$$f(\mathbf{z}(k)) = \frac{1}{\pi^{N_s} \det(R)} \exp(-\mathbf{z}^H(k) R^{-1} \mathbf{z}(k)) \quad (5)$$

where R denotes the correlation matrix of $\mathbf{z}(k)$, which, by using (2) and by observation, can be written in the form

$$\begin{aligned} R &= E[\mathbf{z}(k) \mathbf{z}^H(k)] \\ &= \begin{bmatrix} \sigma_s^2 + \sigma_n^2 & \sigma_s^2 e^{-j\epsilon'} & \dots & \sigma_s^2 e^{-j(N_s-1)\epsilon'} \\ \sigma_s^2 e^{j\epsilon'} & \sigma_s^2 + \sigma_n^2 & \dots & \sigma_s^2 e^{-j(N_s-2)\epsilon'} \\ \vdots & \vdots & \ddots & \vdots \\ \sigma_s^2 e^{j(N_s-1)\epsilon'} & \sigma_s^2 e^{j(N_s-2)\epsilon'} & \dots & \sigma_s^2 + \sigma_n^2 \end{bmatrix} \\ &= \sigma_n^2 I + \sigma_s^2 \mathbf{q} \mathbf{q}^H \quad (6) \end{aligned}$$

where $\mathbf{q} = [1, e^{j\epsilon'}, \dots, e^{j(N_s-1)\epsilon'}]^T$ and I is the identity matrix having the same dimension as the matrix R . Then, we can directly obtain the matrix determinant $\det(R) = (\sigma_n^2)^{N_s-1} (\sigma_n^2 + N_s \sigma_s^2)$ and R^{-1} using the matrix inversion lemma [15], yielding

$$R^{-1} = \frac{1}{\sigma_n^2} I - \frac{\sigma_s^2}{\sigma_n^2 (\sigma_n^2 + N_s \sigma_s^2)} \mathbf{q} \mathbf{q}^H. \quad (7)$$

Equation (5), therefore, becomes

$$\begin{aligned} f(\mathbf{z}(k)) &= \frac{1}{\pi^{N_s} (\sigma_n^2)^{N_s-1} (\sigma_n^2 + N_s \sigma_s^2)} \exp \\ &\quad \times \left[-\frac{1}{\sigma_n^2} \mathbf{z}^H(k) \mathbf{z}(k) + \frac{\sigma_s^2}{\sigma_n^2 (\sigma_n^2 + N_s \sigma_s^2)} \mathbf{z}^H(k) \mathbf{q} \mathbf{q}^H \mathbf{z}(k) \right]. \quad (8) \end{aligned}$$

By simple manipulation, we obtain

$$\begin{aligned} \mathbf{z}^H(k) \mathbf{q} \mathbf{q}^H \mathbf{z}(k) &= \sum_{m=0}^{N_s-1} |r(k+mL_s)|^2 \\ &\quad + \sum_{m=1}^{N_s-1} \sum_{p=m}^{N_s-1} 2 \operatorname{Re} \left\{ r(k+(p-m)L_s) r^*(k+pL_s) e^{jm\epsilon'} \right\} \\ &= \mathbf{z}^H(k) \mathbf{z}(k) + 2 \sum_{m=1}^{N_s-1} \operatorname{Re} \left\{ \gamma_m(k) e^{jm\epsilon'} \right\} \quad (9) \end{aligned}$$

where the superscript $*$ denotes the complex conjugate operation and $\gamma_m(k) = \sum_{p=m}^{N_s-1} r(k+(p-m)L_s)r^*(k+pL_s)$. Substituting (9), (8), and (4) into (3) and rearranging, we obtain the following log-likelihood function

$$\Lambda(\theta, \epsilon) = \sum_{k=\theta}^{\theta+L_s-1} \left\{ \ln c_1 + 2c_2 \sum_{m=1}^{N_s-1} \operatorname{Re} \left\{ \gamma_m(k) e^{jm\epsilon'} \right\} - c_3 \mathbf{z}^H(k) \mathbf{z}(k) \right\} + \sum_{k=1}^L \ln f(r(k)) \quad (10)$$

where $c_1 = ((\sigma_n^2 + \sigma_s^2)^{N_s}) / ((\sigma_n^2)^{N_s-1} (\sigma_n^2 + N_s \sigma_s^2))$, $c_2 = \sigma_s^2 / (\sigma_n^2 (\sigma_n^2 + N_s \sigma_s^2))$, $c_3 = ((N_s - 1) \sigma_s^4) / (\sigma_n^2 (\sigma_n^2 + N_s \sigma_s^2) (\sigma_n^2 + \sigma_s^2))$. The first term $\ln c_1$ and the last term $\sum_{k=1}^L \ln f(r(k))$ are independent of θ and ϵ ; the ML estimate $(\hat{\theta}_{\text{ML}}, \hat{\epsilon}_{\text{ML}})$, therefore, is given by

$$\hat{\theta}_{\text{ML}}, \hat{\epsilon}_{\text{ML}} = \arg \max_{\theta, \epsilon} \sum_{k=\theta}^{\theta+L_s-1} \left[\sum_{m=1}^{N_s-1} \operatorname{Re} \left\{ \gamma_m(k) e^{jm\epsilon'} \right\} - \frac{N_s - 1}{2} \rho \mathbf{z}^H(k) \mathbf{z}(k) \right] \quad (11)$$

where $\rho = \sigma_s^2 / (\sigma_n^2 + \sigma_s^2)$. Note that for $N_s = 2$, (11) is equal to the (5) in [8], as expected.

A. Cramér–Rao Bound for Frequency-Offset Estimate

If the time offset has been given *a priori* and assume the estimation of frequency offset is unbiased, then its Cramér–Rao bound can be derived directly using the result [18]

$$\mathbb{E} [(\hat{\epsilon}(\mathbf{r}) - \epsilon)^2] \geq \left\{ -\mathbb{E} \left[\frac{\partial^2 \ln f(\mathbf{r}|\theta, \epsilon)}{\partial \epsilon^2} \right] \right\}^{-1}. \quad (12)$$

Note that extensive simulations have shown that the frequency estimate via the ML algorithm (11) is unbiased, but this property has not been analytically proven, and hence the assumption is made. Taking the second derivative of the log-likelihood function with respect to ϵ using (10), we obtain

$$\frac{\partial^2 \ln f(\mathbf{r}|\theta, \epsilon)}{\partial \epsilon^2} = \sum_{k=\theta}^{\theta+L_s-1} -2c_2 \left(\frac{2\pi L_s}{N} \right)^2 \sum_{m=1}^{N_s-1} \sum_{p=m}^{N_s-1} m^2 \operatorname{Re} \left\{ r(k+(p-m)L_s) r^*(k+pL_s) e^{jm\epsilon'} \right\}. \quad (13)$$

We then apply the expectation, use results in (2), and replace c_2 by its value, yielding

$$\begin{aligned} & -\mathbb{E} \left[\frac{\partial^2 \ln f(\mathbf{r}|\theta, \epsilon)}{\partial \epsilon^2} \right] \\ &= 2c_2 \left(\frac{2\pi L_s}{N} \right)^2 \sum_{k=\theta}^{\theta+L_s-1} \sum_{m=1}^{N_s-1} \sum_{p=m}^{N_s-1} m^2 \\ & \quad \times \operatorname{Re} \left\{ \mathbb{E} [r(k+(p-m)L_s) r^*(k+pL_s)] e^{jm\epsilon'} \right\} \\ &= \frac{8\pi^2 L_s^3 \sigma_s^4}{N^2 \sigma_n^2 (\sigma_n^2 + N_s \sigma_s^2)} \sum_{m=1}^{N_s-1} m^2 (N_s - m) \\ &= \frac{2\pi^2 L_s^3 N_s^2 (N_s - 1) \sigma_s^4}{3N^2 \sigma_n^2 (\sigma_n^2 + N_s \sigma_s^2)}. \end{aligned} \quad (14)$$

The Cramér–Rao bound, therefore, is obtained

$$\mathbb{E} [(\hat{\epsilon}(\mathbf{r}) - \epsilon)^2] \geq \frac{3N^2 \sigma_n^2 (\sigma_n^2 + N_s \sigma_s^2)}{2\pi^2 L_s^3 N_s^2 (N_s - 1) \sigma_s^4}. \quad (15)$$

This bound is intuitive; when the number of identical data set N_s or the number of data samples in each set L_s increases, the bound decreases. The bound also shows the advantage of using multiple sets instead of two sets of identical data for frequency-offset estimation.

III. SIMPLIFIED ALGORITHM

The computational complexity to realize (11) for estimating θ, ϵ is intensive because a two-dimensional searching is required. Here, we present a simplified algorithm for reducing the realization complexity. Let $\angle x$ denote the angle of x . Then, the likelihood function (11) is maximized if the frequency offset ϵ given θ_{ML} makes $\angle[\sum_{k=\theta_{\text{ML}}}^{\theta_{\text{ML}}+L_s-1} \gamma_m(k) + m\epsilon'] = 0$ for all $m = 1, \dots, N_s - 1$. The simplified algorithm presumes first that the frequency-offset estimate makes $\angle[\sum_{k=\theta_{\text{ML}}}^{\theta_{\text{ML}}+L_s-1} \gamma_m(k) + m\epsilon'] = 0$ for $m = 1, \dots, N_s - 1$. Note that this presumption can be true for $N_s = 2$ but is generally impossible to attain for $N_s > 2$. This discrepancy, therefore, makes the simplified algorithm result in a performance loss for $N_s > 2$. The time offset, using (11) under the presumption, can then be estimated by the following equation:

$$\begin{aligned} & \hat{\theta}_{\text{ML}, \text{sim}} \\ &= \arg \max_{\theta} \sum_{k=\theta}^{\theta+L_s-1} \left\{ \sum_{m=1}^{N_s-1} \operatorname{Re} \left\{ \gamma_m(k) e^{jm\epsilon'} \right\} - \frac{N_s - 1}{2} \rho \mathbf{z}^H(k) \mathbf{z}(k) \right\} \\ &= \arg \max_{\theta} \left\{ \sum_{m=1}^{N_s-1} \left| \sum_{k=\theta}^{\theta+L_s-1} \gamma_m(k) \right| - \sum_{k=\theta}^{\theta+L_s-1} \frac{N_s - 1}{2} \rho \mathbf{z}^H(k) \mathbf{z}(k) \right\}. \end{aligned} \quad (16)$$

The obtained time-offset estimate, via the above equation, is used to find the frequency offset. For each index m , we obtain, from the presumed condition, one estimate $\hat{\epsilon}^m = -\angle[\sum_{k=\hat{\theta}_{\text{ML}, \text{sim}}}^{\hat{\theta}_{\text{ML}, \text{sim}}+L_s-1} \gamma_m(k)]/m$. These $N_s - 1$ frequency-offset estimates are then averaged to yield the final estimate

$$\hat{\epsilon}_{\text{ML}, \text{sim}} = \frac{-N}{2\pi L_s (N_s - 1)} \sum_{m=1}^{N_s-1} \frac{1}{m} \angle \left[\sum_{k=\hat{\theta}_{\text{ML}, \text{sim}}}^{\hat{\theta}_{\text{ML}, \text{sim}}+L_s-1} \gamma_m(k) \right]. \quad (17)$$

The complexity to realize the algorithm (16), (17) takes approximately $N_s^2 L_s K_\theta$ operations (including multiplication, addition, and arc-tangent operations), where K_θ denotes the range of θ for searching while to realize the ML algorithm (11) requires approximately $N_s^2 L_s K_\theta K_\epsilon$ operations, where K_ϵ is the number to partition the frequency offset for searching. Therefore, the realization complexity of the simplified algorithm is greatly reduced. The frequency-offset estimator in (17) can be analytically shown to be consistent if the time-offset $\hat{\theta}_{\text{ML}, \text{sim}}$ is properly chosen. For brevity, we only describe the proof procedure. For the received data in the preamble set, the product $r(k)r^*(k+mL_s)$ is an addition of a constant multiplying a random variable which is chi-square distributed with two degrees

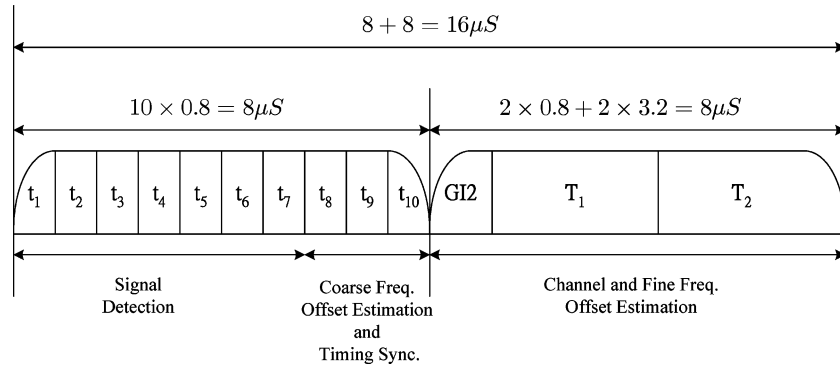


Fig. 2. Structure of the IEEE 802.11a preamble.

of freedom and three zero-mean Gaussian random variables, as seen from the following equation:

$$r(k)r^*(k+mL_s) = |s(k-\theta)|^2 e^{-jm\epsilon'} + n(k)s^*(k-\theta) + n^*(k+mL_s)s(k-\theta) + n(k)n^*(k+mL_s). \quad (18)$$

Since $\gamma_m(k) = \sum_{p=m}^{N_s-1} r(k+(p-m)L_s)r^*(k+pL_s)$, the random variable $\gamma_m(k)$, therefore, is an addition of a random variable with the chi-square distribution of higher degrees of freedom and more Gaussian random variables. Therefore, as the number of preamble data is increased, both the averaged imaginary part and the averaged real part of $\gamma_m(k)$, by the statistical properties of both the chi-square and the Gaussian distributions, converge to a constant multiplying $\sin(2m\pi\epsilon')$ and $\cos(2m\pi\epsilon')$, respectively. The variance of each also converges to zero. The ratio then converges to the desired value $\tan(2m\pi\epsilon')$ with its variance also converging to zero; hence, the consistency of the time-offset estimator is obtained.

Note that for $N_s = 2$, this simplified algorithm is just the exact ML algorithm, which has been derived in [8]. For $N_s > 2$, however, the solutions using the simplified algorithm are no longer the ML estimates. The simplified algorithm, therefore, reduces the realization complexity at the cost of modest performance degradation, as illustrated by the simulation results in the following section.

IV. SIMULATIONS

The IEEE 802.11a standard defines the preamble as illustrated in Fig. 2. Each preamble consists of ten identical short symbols and two identical long symbols. Note that the ten short symbols and the two long symbols can be combined together by using the method similar to the second approach proposed in [9] for performance improvement. For demonstration and for simplicity, here we only use the ten repeated short symbols for the estimation of time and frequency offsets. The number of subcarriers in IEEE 802.11a is $N = 64$, and the sampling frequency is 20 MHz. One short symbol is of duration $0.8 \mu s$ and hence has 16 samples.

Monte Carlo simulations are used to evaluate the performance of the proposed algorithms in both AWGN and dispersive channels. The dispersive channel, similar to the model used in [8], has 15 independent Rayleigh-fading taps with an exponentially decaying power delay profile of the root mean-squared width equal to $0.1 \mu s$ (two samples) and the maximum delay spread of $0.75 \mu s$ (15 samples). The signal-to-noise ratio (SNR) is measured at the received signal. The squared estimation errors of the frequency offset and the time offset, averaged over 1000 trials, versus SNRs at 0, 1, to 10 dB, are shown in Figs. 3 and 4, respectively. These results show that the performance of the proposed algorithms, as expected, degrades for the dispersive channel because the transmitted signals passed through the channel result in signals

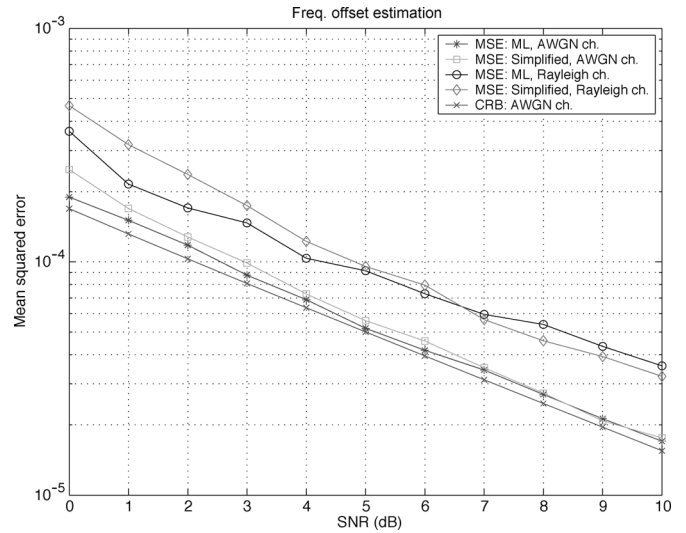


Fig. 3. Mean-squared error of the frequency-offset estimate versus SNRs.

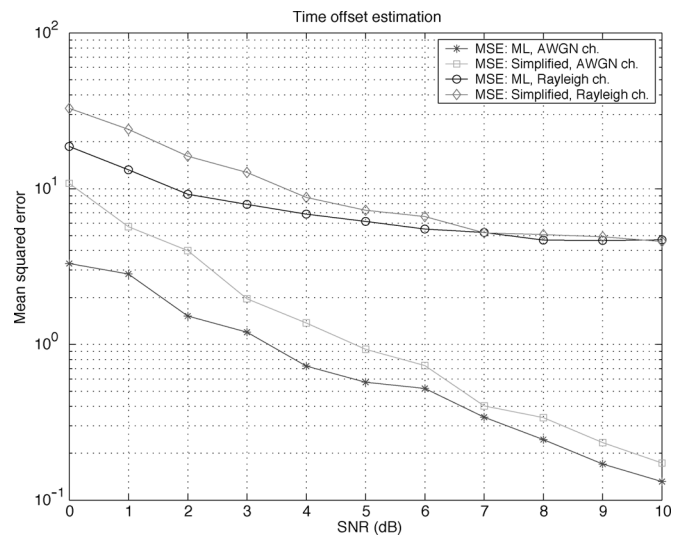


Fig. 4. Mean-squared error of the time-offset estimate versus SNRs.

which are no longer uncorrelated. The performance of the simplified algorithm at low SNRs, as shown in the figures, is slightly worse than that of the ML method but its difference is decreasing as the SNR is increasing. The simplified algorithm, although inferior to the ML algorithm in performance, is more practical when the realization complexity is concerned.

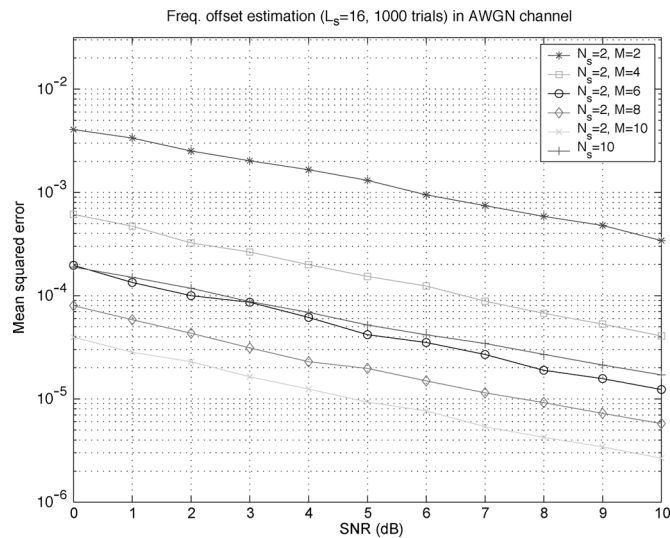


Fig. 5. Comparison of the frequency-offset estimator between the approach [8] and the proposed method.

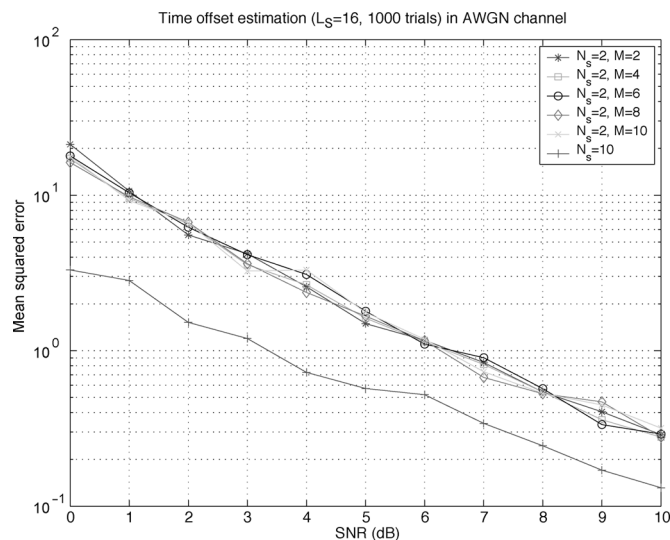


Fig. 6. Comparison of the time-offset estimator between the approach [8] and the proposed method.

Simulations are also performed for performance comparison between the proposed approach and that in [8]. For simplicity, we only demonstrate the simulation results in AWGN channels even the tendency in dispersive channels is also similar. The proposed algorithm uses ten sets of identical data ($N_s = 10$), with each set having 16 samples ($L_s = 16$), while the approach in [8] uses two sets of identical data ($\bar{N}_s = 2$), with each set having $\bar{L}_s = M L_s$ samples, where M is an integer. It has been shown in [9] that the estimator using two sets of identical data with each set having \bar{L}_s samples is equivalent in performance to the estimator using M symbols, with each symbol having the cyclic prefix of length L_s . The estimates of the frequency offset and the time offset, averaged over 1000 trials versus SNRs are shown in Figs. 5 and 6, respectively. These results demonstrate that the symbol number M has little effect on the time-offset estimator but influences significantly the performance of frequency-offset estimation. Note that the proposed approach and the method in [8] are closely comparable in the performance of frequency-offset estimation when $M = 6$. In fact, this number can be derived because the performance of each algorithm can be approximated by the obtained Cramér–Rao bound (15). In terms of (15), under the assumption of the same SNR

and the same number of OFDM subcarriers, two approaches attain the same Cramér–Rao bound if the following equation is satisfied:

$$\frac{N_s^2 (N_s^2 - 1) L_s^3}{NSR + N_s} = \frac{\bar{N}_s^2 (\bar{N}_s^2 - 1) \bar{L}_s^3}{NSR + \bar{N}_s} \quad (19)$$

where $NSR = \sigma_n^2 / \sigma_s^2$. For example, if $NSR = 1$ (0 dB SNR), $N_s = 10$ and $\bar{N}_s = 2$, then $M = \bar{L}_s / L_s = 6.0822$; this solution matches well with the simulation result. Hence, the length of the cyclic prefix should be about six times the length of one identical set such that the approach [8] can attain the same performance as our method.

V. CONCLUSION

We have derived an ML algorithm for the estimation of frequency and time offsets in OFDM systems using multiple sets of identical data; the Cramér–Rao bound for the frequency offset is also obtained. We have further developed a simplified algorithm for reducing the realization complexity. Simulations using the preamble data in IEEE 802.11a standard have been performed to verify the effectiveness of the proposed algorithms.

REFERENCES

- [1] J. A. C. Bingham, "Multicarrier modulation for data transmission: An idea whose time has come," *IEEE Commun. Mag.*, vol. 28, no. 5, pp. 5–14, May 1990.
- [2] W. Y. Zou and Y. Wu, "COFDM: An overview," *IEEE Trans. Broadcast.*, vol. 41, no. 1, pp. 1–8, Mar. 1995.
- [3] J. S. Chow, J. C. Tu, and J. M. Cioffi, "A discrete multitone transceiver system for HDSL applications," *IEEE J. Sel. Areas Commun.*, vol. 9, no. 6, pp. 895–908, Aug. 1991.
- [4] P. H. Moose, "A technique for orthogonal frequency division multiplexing frequency offset correction," *IEEE Trans. Commun.*, vol. 42, no. 10, pp. 2908–2914, Oct. 1994.
- [5] T. Pollet, M. V. Bladel, and M. Moeneclaey, "BER sensitivity of OFDM systems to carrier frequency offset and Wiener phase noise," *IEEE Trans. Commun.*, vol. 43, no. 2/3/4, pp. 191–193, Feb./Mar./Apr. 1995.
- [6] S. Chang and E. J. Powers, "Efficient frequency-offset estimation in OFDM-based WLAN systems," *IEE Electron. Lett.*, vol. 39, no. 21, pp. 1554–1555, Oct. 2003.
- [7] J. Li, G. Liu, and G. B. Giannakis, "Carrier frequency offset estimation for OFDM-based WLANs," *IEEE Signal Process. Lett.*, vol. 8, no. 3, pp. 80–82, Mar. 2001.
- [8] J.-J. van de Beek, M. Sandell, and P. O. Börjesson, "ML estimation of time and frequency offset in OFDM systems," *IEEE Trans. Signal Process.*, vol. 45, no. 7, pp. 1800–1805, Jul. 1997.
- [9] J.-J. van de Beek, P. O. Börjesson, M.-L. Boucheret, D. Landström, J. M. Arenas, P. Ödling, and S. K. Wilson, "Three nonpilot based time- and frequency estimators for OFDM," *Elsevier's Signal Processing (Special Issue on COST 254 Workshop)*, vol. 80, no. 7, Jul. 2000.
- [10] H. Bölcskei, "Blind estimation of symbol timing and carrier frequency offset in wireless OFDM systems," *IEEE Trans. Commun.*, vol. 49, no. 6, pp. 988–999, Jun. 2001.
- [11] H. Meyr and G. Ascheid, *Synchronization in Digital Communications: Phase-, Frequency-Locked Loops, and Amplitude Control*. New York: Wiley, 1990, vol. 1–2.
- [12] H. Meyr, M. Moeneclaey, and S. A. Fechtel, *Digital Communication Receivers, Synchronization, Channel Estimation, Signal Processing*. New York: Wiley, 1998.
- [13] U. Mengali and A. N. D'Andrea, *Synchronization Techniques for Digital Receivers*. New York: Plenum, 1997.
- [14] *Wireless LAN Medium Access Control (MAC) and Physical Layer (PHY) Specifications: High-Speed Physical Layer in the 5 GHz Band*, IEEE Standard 802.11a, Dec. 1999.
- [15] G. H. Golub and C. F. V. Loan, *Matrix Computation*, 2nd ed. Baltimore, MD: The Johns Hopkins Univ. Press, 1989.
- [16] T. Pollet, P. Spruyt, and M. Moeneclaey, "The BER performance of OFDM systems using nonsynchronized sampling," *Proc. IEEE GLOBECOM*, vol. 1, pp. 253–257, Nov. 1994.
- [17] K. S. Miller, *Complex Stochastic Processes, An Introduction to Theory and Application*. Reading, MA: Addison-Wesley, 1974.
- [18] H. L. Van Trees, *Detection, Estimation, and Modulation Theory*. New York: Wiley, 1968.